Available online at www.sciencedirect.com
ScienceDirect
Tetrahedron 62 (2006) 10408–10416
Tetrahedron

A DFT study for the formation of imidazo[1,2-*c*]pyrimidines through an intramolecular Michael addition

Luis R. Domingo,[a,*] José A. Sáez,[a] Cristina Palmucci,[a] José Sepúlveda-Arques[b] and M. Eugenia González-Rosende[c]

[a] *Departamento de Química Orgánica, ICMOL, Universidad de Valencia, Dr. Moliner 50, 46100 Burjassot, Valencia, Spain*
[b] *Departamento de Química Orgánica, Universidad de Valencia, Avda. Vicent Andrés Estellés s/n, 46100 Burjassot, Valencia, Spain*
[c] *Departamento de Química, Bioquímica y Biología Molecular, Universidad Cardenal Herrera-CEU, 46113 Moncada, Valencia, Spain*

Received 3 July 2006; revised 14 August 2006; accepted 18 August 2006
Available online 7 September 2006

Abstract—The formation of imidazo[1,2-*c*]pyrimidines through a ring closure of 2-(2-sulfonylimino-1,2-dihydro-1-pyrimidinyl) acetamides has been studied using DFT methods. Analysis of the energy results for the cyclization step shows the demand of almost an acid catalyst, which increases the electrophilicity of the dihydropyrimidine moiety, in order to make feasible the intramolecular Michael addition. The substitution on both dihydropyrimidine and amide moieties has also an influence on the cyclization step.

1. Introduction

In a previous paper, we reported the synthesis of a series of imidazo[1,2-*a*]pyrimidines **4** using 2-tosylaminopyrimidines **1** as starting materials.[1] The alkylation of **1A** with 2-bromoacetamides **2a**–**f** and the alkylation of **1B**,**C** with 2-bromoacetamide **2a** afforded the corresponding dihydropyrimidines **3** that were converted into the target products **4** with trifluoroacetic anhydride. Nevertheless, the reaction of pyrimidines **1B**,**C** with 2-bromoacetamides **2b**–**f** afforded the hexahydroimidazo[1,2-*c*]pyrimidines **5** (Scheme 1).[1]

Several methods have been applied for the synthesis of imidazo[1,2-*c*]pyrimidines and the most frequently developed procedure involves the condensation of 4(6)-aminopyrimidine derivatives.[2] To the best of our knowledge, our finding was the first example of a synthesis of imidazo[1,2-*c*]pyrimidines starting from 2-aminopyrimidines and constitutes

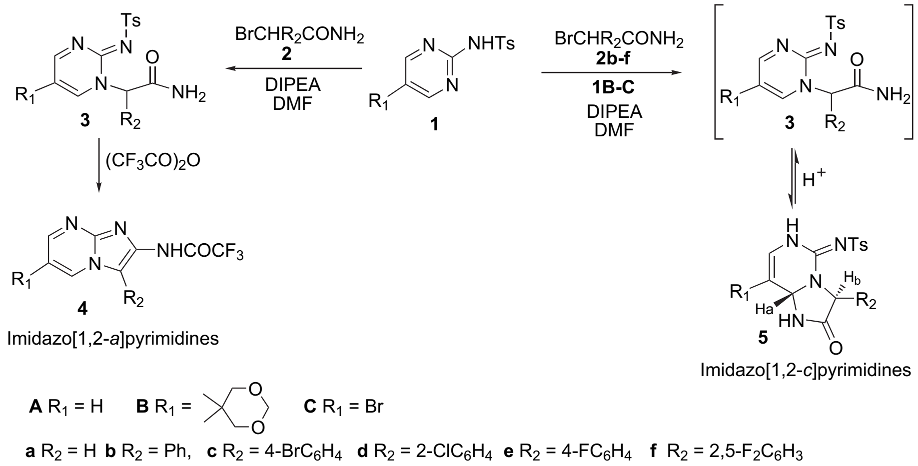

Scheme 1.

Keywords: Pyrimidines; Cyclization; Michael addition; Electrophilicity; DFT calculations.

* Corresponding author. Fax: +34 96 354 3106; e-mail: domingo@utopia.uv.es

doi:10.1016/j.tet.2006.08.066

a novel synthetic method for these compounds. The formation of the imidazo[1,2-*c*]pyrimidines **5** is the result of an intramolecular Michael addition of the carboxamide group to the α,β-unsaturated imine system. The detection of the open ring alkylated product **3Be**, by ^{13}C NMR, when imidazopyrimidine **5Be** was stirred with catalytic amounts of *p*-toluenesulfonic acid, showed that the attack of the carboxamide group to the α,β-unsaturated imine is a reversible reaction. The structure of the compound **5Ac** was determined by X-ray crystallography.[1] The trans disposition of the H_a and H_b hydrogens of the imidazopyrimidine **5Ac** confirmed that the addition of the amide to the unsaturated imine is diastereoselective with the nucleophilic attack occurring preferentially on the opposite face to the aryl group present on the amide substituent (Scheme 1). The formation of the hexahydroimidazo[1,2-*c*]pyrimidines **5** as major products only in the case of pyrimidines with R_1 and R_2 different from H was initially attributed to steric factors that induce a favorable conformation for the ring closure. However, they can be also obtained from unsubstituted sulfonamidopyrimidines **2A**. In fact, when the alkylated product **3Ac**, obtained from **1A** and **2c**, was stored in THF solution at room temperature for a week in the presence of catalytic amounts of diisopropylethylamine (DIPEA), the corresponding product **5Ac** was obtained (20%).

The nucleophilic attack of a carboxamide group to an α,β-unsaturated system is not very frequent and there are few references reported in the literature. The most common examples are intramolecular nucleophilic additions of a carboxamide group to strongly electrophilic iminium species, derived from the reaction of amino groups with aldehydes or ketones under acidic conditions[3] or dichloromethane[4] (Scheme 2). An example of an intermolecular addition was reported for the synthesis of the rolitetracycline.[5]

In the present paper, we have carried out a theoretical study for the cyclization reaction of the 2-(2-sulfonylimino-1,2-dihydro-1-pyrimidinyl) acetamides **3** with the formation of the hexahydroimidazo[1,2-*c*]pyrimidines **5**, using DFT methods at the B3LYP/6-31G* level. Two reaction models have been chosen. The first one corresponds to the cyclization of the iminium cation **6** (see Scheme 3). The second one corresponds to the formation of hexahydroimidazo[1,2-*c*]pyrimidines **5** through an intramolecular Michael addition. Finally, a DFT analysis based on the global reactivity indexes of the reactants involved in these intramolecular processes will be performed. Our main interest is to explain the participation of these dihydropyrimidyl acetamides in intramolecular Michael additions.

2. Computational methods

DFT calculations were carried out using the B3LYP[6] exchange-correlation functionals, together with the standard 6-31G* basis set.[7] The optimizations were carried out using the Berny analytical gradient optimization method.[8] The stationary points were characterized by frequency calculations in order to verify that the transition structures (TSs) have one and only one imaginary frequency. Inclusion of thermal corrections to enthalpies and entropies (computed at 25 °C and 1 atm) to the energies, increases the activation free energies for the intermolecular Michael additions in a narrow range from 0.4 to 1.0 kcal/mol. Thus, energy discussions will be made on the basis of the relative energies. The intrinsic reaction coordinate (IRC)[9] path was traced in order to check the energy profiles connecting each TS to the two associated minima of the proposed mechanism by using the second-order González–Schlegel integration method.[10] The electronic structures of stationary points were analyzed by the NBO method.[11] All calculations were carried out with the Gaussian 03 suite of programs.[12]

These reactions are carried out in polar solvents, and as solvent can modify the gas-phase activation energy, their effects have been studied. The solvent effects have been considered by B3LYP/6-31G* single point calculations on the gas-phase stationary points using a relatively simple self-consistent reaction field (SCRF) method[13] based on the polarizable continuum model (PCM) of the Tomasi's group.[14] The solvent used in the experimental work is dimethylformamide (DMF), ε=38.25. We have used dimethylsulfoxide (DMSO), which has also a large dielectric constant, ε=46.7.

The global electrophilicity index,[15] ω, which measures the stabilization energy when the system acquires an additional electronic charge ΔN from the environment, has been given by the following simple expression,[15] $\omega=(\mu^2/2\eta)$, in terms of the electronic chemical potential μ and the chemical hardness η. Both quantities may be approached in terms of the one electron energies of the frontier molecular orbital HOMO and LUMO, ε_H and ε_L, as $\mu \approx (\varepsilon_H+\varepsilon_L)/2$ and $\eta \approx (\varepsilon_L-\varepsilon_H)$, respectively.[16]

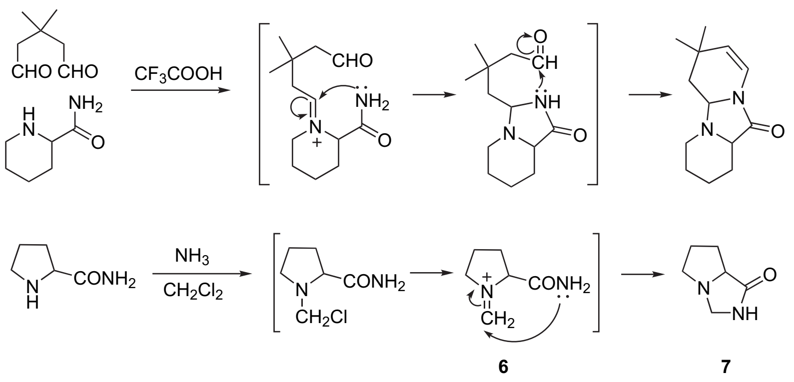

Scheme 2.

3. Results and discussions

3.1. Study of the cyclization reaction of the iminium cation 6

Firstly, the cyclization reaction of the iminium cation **6** was studied. This cyclization reaction is a one-step process associated with the nucleophilic attack of the amide N3 nitrogen atom to the iminium C2 carbon atom with formation of the C2–N3 bond (see Scheme 3). Therefore, the iminium cation **6**, the TS associated with the nucleophilic attack, **TS1**, and the intermediates **8** and **9** were located and characterized. The total energies in gas-phase and in DMSO are summarized in Table 1, while a schematic representation for the reaction profile of this cyclization is given in Figure 1.

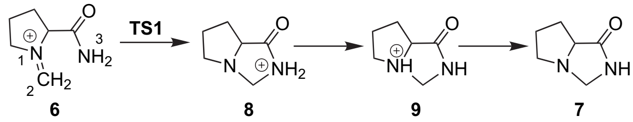

Scheme 3.

Since some paths involve TSs and intermediates with charges, and solvent effects can stabilize these species, the energetic discussion will be performed using the energies obtained in DMSO. The activation energy associated with the nucleophilic attack of the amide N3 nitrogen atom to the iminium C2 carbon atom with the formation of the five-membered heterocycle is 21.4 (25.0) kcal/mol (energies in parenthesis correspond to the gas-phase calculations). Formation of the intermediate **8** is endothermic in 13.6 (20.5) kcal/mol. However, a proton transfer process from the amide N3 nitrogen atom to the amine N1 nitrogen atom converts the intermediate **8** into **9**, which is 24.8 (20.5) kcal/mol more stable (see Fig. 1). This large stabilization is related to the more basic character of the amine N1 nitrogen atom than the amide N3 one. Finally, an acid/base reaction will transform **9** into the final product **7**.

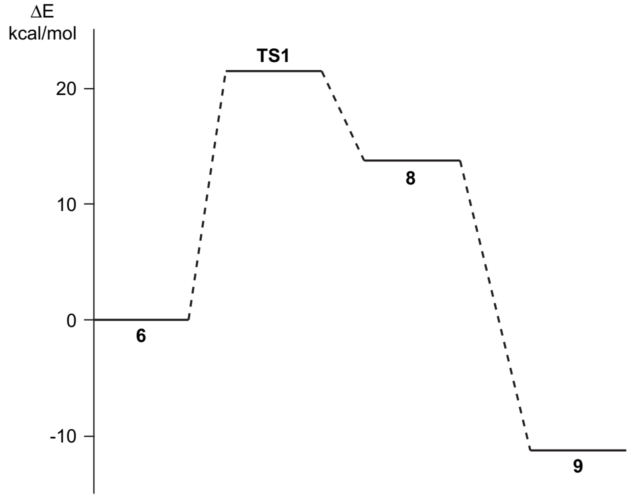

Figure 1. Reaction profile, in DMSO, for the cyclization reaction of the iminium cation **6**.

The geometry of **TS1** is given in Figure 2. The length of the C2–N3 forming bond at **TS1** is 1.967 Å, while at the intermediates **8** and **9** this length is 1.612 and 1.424 Å, respectively. The extent of bond-formation along a reaction pathway is provided by the concept of bond order (BO).[17] The BO value of the C2–N3 forming bond at **TS1** is 0.44, while the N1–C2 BO value is 1.37.

3.2. Study of the transformation of the 2-mesylaminopyrimidines 10 into imidazo[1,2-*c*]pyrimidines 15

The transformation of the 2-mesylaminopyrimidines **10** into imidazo[1,2-*c*]pyrimidines **15** requires two consecutive reactions: (i) the first one is a nucleophilic substitution of the 2-bromoacetamide derivatives **12** by the 2-mesylaminopyrimidines **11**, which are obtained by deprotonation of **10**, to give the *N*-substituted dihydropyrimidines **13**; (ii) the second reaction is a cyclization reaction of the dihydropyrimidines **13** to give the zwitterionic intermediate **14**, which by an acid/base process gives **15** (see Scheme 4). For these

Table 1. B3LYP/6-31G* total energies (in au) in gas-phase and in DMSO for the stationary points involved in the cyclization reactions of the iminium cation **6** and the dihydropyrimidines **13a–c**

	In gas-phase	In DMSO		In gas-phase	In DMSO
6	−419.754306	−419.841906	**18a**	−1115.950536	−1116.045935
TS1	−419.714505	−419.807827	**18b**	−1346.994052	−1347.089565
8	−419.721655	−419.820269	**18c**	−1653.477152	−1653.565623
9	−419.754241	−419.859759	**TS5a**	−1115.899471	−1116.006436
11a	−907.019956	−907.117406	**TS5b**	−1346.954958	−1347.055554
11b	−907.019956	−907.117406	**TS5c**	−1653.441006	−1653.530485
11c	−1213.493973	−1213.595640	**TS6a**	−1115.896746	−1116.005921
12a	−2780.315365	−2780.328801	**TS6b**	−1346.944796	−1347.045044
12b	−3011.366853	−3011.384590	**19a**	−1115.895976	−1116.008533
12c	−3011.366853	−3011.384590	**19b**	−1346.956359	−1347.059178
TS2a	−3687.327589	−3687.428311	**19c**	−1653.443485	−1653.536675
TS2b	−3918.379001	−3918.480054	**20a**	−1115.899883	−1116.009713
TS2c	−4224.861350	−4224.960196	**20b**	−1346.956628	−1347.061592
13a[a]	−3687.377833	−3687.484147	**20c**	−1653.448134	−1653.539694
13b[a]	−3918.426477	−3918.529842	**21a**	−1115.897050	−1116.008856
13c[a]	−4224.890958	−4225.007929	**21b**	−1346.948691	−1347.055303
16	−1695.979992	−1696.060038			
TS4	−1695.944237	−1696.019777			
17	−1696.007098	−1696.070158			

[a] Compound **13** plus Br^- total energies.

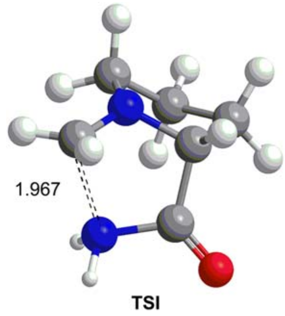

Figure 2. Transition structure, **TS1**, associated with the cyclization of the iminium cation **6**. The distance is given in Å.

reactions, three computational models have been considered, which are related to the X (H or dioxane) and Y (H or Ph) substitutions on the pyrimidine and the acetamide moieties, respectively (*Model I* (X=H, Y=H), *Model II* (X=H, Y=Ph), and *Model III* (X=dioxane, Y=Ph)). In these computational models, the experimental *p*-toluenesulfonyl group has been substituted by the methanesulfonyl one.

3.2.1. Nucleophilic substitutions on the 2-bromoacetamides derivatives 12.

The attachment of the acetamide on the 2-mesylaminopyrimidines **10** is carried out by a nucleophilic attack of the latter to the corresponding 2-bromoacetamide derivative **12**, to afford the dihydropyrimidines **13** (see Scheme 4). The total energies in gas-phase and in DMSO are summarized in Table 1, while a schematic representation for the reaction profiles of these nucleophilic substitutions is given in Figure 3.

The activation energies for the nucleophilic attacks of **11** to **12** are 11.2 (4.9) kcal/mol for *Model I*, 13.8 (4.9) kcal/mol for *Model II*, and 12.6 (−0.3) kcal/mol for *Model III* (see Fig. 3). These low values make the substitution reaction on the α position of the carboxamide group very favorable. Note that, in gas-phase, **TS2c** is located below reagents; however, the inclusion of diffuse functions by single point calculation at the B3LYP/6-31+G* level makes its barrier slightly positive (0.49 kcal/mol). These reactions are exothermic in −17 to −24 (−19 to −27) kcal/mol. Therefore, formation of the dihydropyrimidines **13** are kinetically and thermodynamically favored process. Inclusion of thermal corrections to enthalpies and entropies to the gas-phase energies, increases the activation free energies for the nucleophilic substitutions in a range from 13.7 to 15.3 kcal/mol, as a consequence of the bimolecular nature of these processes.

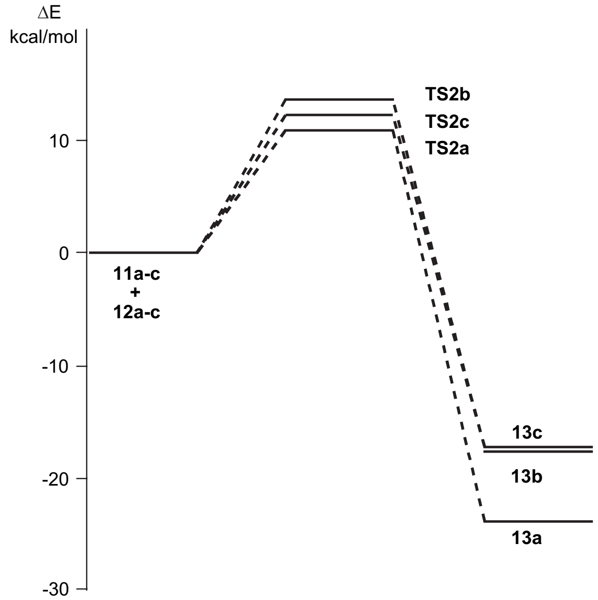

Figure 3. Reaction profiles, in DMSO, for the nucleophilic substitutions on the 2-bromoacetamides derivatives **12a–c**.

The geometries of the TSs are given in Figure 4. The lengths of the N2–C5 forming and C5–Br breaking bonds at the TSs are 1.954 and 2.626 Å at **TS2a**, 1.973 and 2.806 Å at **TS2b**, and 2.102 and 2.658 Å at **TS2c**, respectively. The N2–C5–Br angle at these TSs are 172.0° at **TS2a**, 169.0° at **TS2b**, and 166.5° at **TS2c**. For these S_N2 reactions there is a deviation of the linear rearrangement with the increase of the substitution on both reagents. The BO values of the N2–C5 forming and C5–Br breaking bonds at the TSs are 0.45 and 0.38 at **TS2a**, 0.46 and 0.25 at **TS2b**, and 0.35 and 0.35 at **TS2c**, respectively. While **TS2a** and **TS2b**, correspond to asynchronous processes where the C5–Br breaking bond is

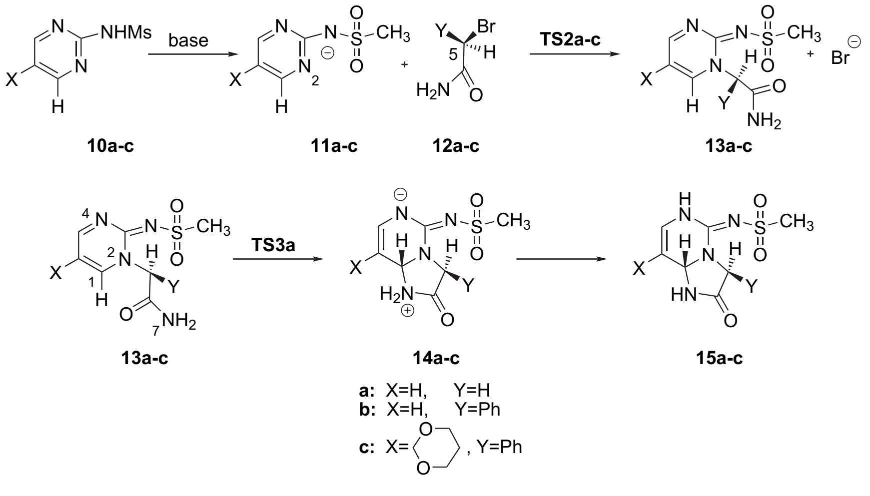

Scheme 4.

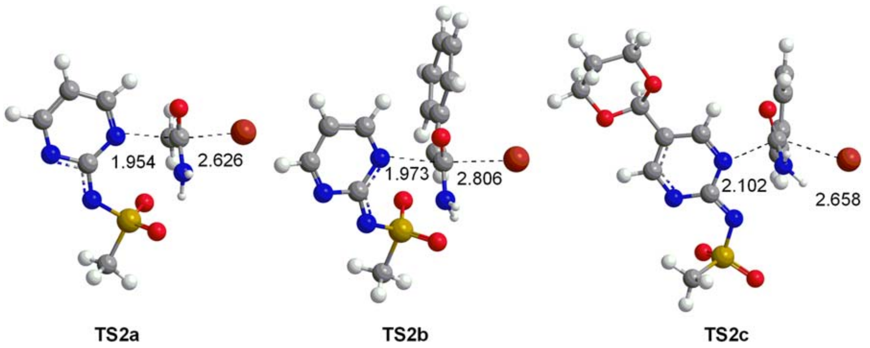

Figure 4. Transition structures, **TS2a–c**, associated with the nucleophilic substitutions on the 2-bromoacetamides derivatives **12a–c**. The distances are given in Å.

more advanced than the N2–C5 forming bond, **TS2c** corresponds to a synchronous process.

3.3. Study of the cyclization reaction of the dihydropyrimidines 13

The cyclization reaction of the dihydropyrimidines **13** to give the imidazo[1,2-*c*]pyrimidines **15** involves an intramolecular Michael addition of the amide N7 nitrogen atom to the C1 conjugate position of **13**. All attempts to locate the TSs and adducts associated with this intramolecular Michael addition at the three models were unsuccessful. Only HF/6-31G* calculations in DMSO allowed to find a TS for the reaction *Model I*, **TS3a**, but it presented a very high activation energy, 41.9 kcal/mol. Further optimizations of this structure at the B3LYP/6-31G* level yielded the dihydropyrimidine **13a**. These unfavorable energy results, which prevent the cyclization process on **13**, can be related to the low electrophilic character of the dihydropyrimidine ring and the low nucleophilic character of the amide residue (see later), as well as to the large energy associated with the formation of the zwitterionic structure **14**.

Then, the cyclization step with formation of the imidazo[1,2-*c*]pyrimidines **15** must take place through an acid/base catalysis. The acid/base catalysis has two favorable roles. While the acid catalysis increases the electrophilicity of the dihydropyrimidine moiety of **13**, favoring the Michael addition, the basic catalysis increases the nucleophilicity of the amide group. To study the effects of the acid/base catalysts in these cyclizations, two molecular models were considered. The first one corresponds to a basic catalysis achieved by the inclusion of a trimethylamine molecule, as a reduced model of DIPEA, hydrogen-bonded to an amide hydrogen atom. However, at DFT level it was not possible to find the TS associated with this base catalyzed cyclization; the energy for this process was estimated in ca. 50 kcal/mol. In addition, all attempts to find the corresponding product were unsuccessful because the ring cleavage to give the dihydropyrimidine **13** takes place without an appreciable barrier. These facts caused to discard the base catalyzed process. The second one is an acid/base catalysis where a trimethylammonium cation was also hydrogen-bonded to the pyrimidine N4 nitrogen atom.

For the acid/base catalyzed cyclization reaction of the *Model II*, both **TS4**, associated with the intramolecular addition by the *re*-face of the planar C1 carbon and the corresponding product **17** were located and characterized (see Scheme 5). The total energies in gas-phase and in DMSO are summarized in Table 1, while a schematic representation for the reaction profile of the acid/base catalyzed reaction is given in Figure 5.

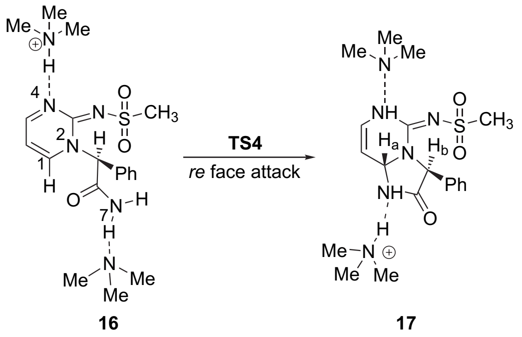

Scheme 5.

The activation energy associated with the acid/base catalyzed intramolecular Michael addition of **16** via **TS4** is 25.3 (22.4) kcal/mol. This energy result suggests that the

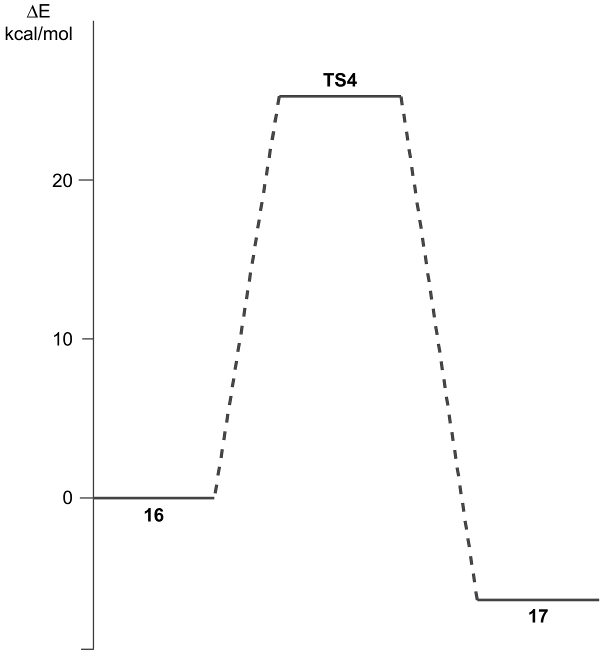

Figure 5. Reaction profile, in DMSO, for the acid/base catalyzed cyclization reaction of the dihydropyrimidine **13b**.

acid catalysis has a relevant role on the cyclization reaction of the dihydropyrimidines **13**, being essential the electrophilic activation of the pyrimidine ring. This value is ca. 4 kcal/mol larger than that obtained for the cyclization of iminium cation **6**, via **TS1**.

The geometry of **TS4** is given in Figure 6. The lengths of the C1–N7 forming bond at the TS of the acid/base catalyzed process is 1.864 Å. At this TS, the length of the amide N7–H breaking and the N4–H forming bonds are 1.098 and 1.632 Å, respectively. The BO value of the C1–N7 forming bond at this TS is 0.52, while the BO values for the amide N7–H breaking and the N4–H forming bonds are 0.60 and 0.18, respectively. In this catalyzed process N7–H breaking bond process is more advanced than the N4–H forming bond one.

Finally, in view of the necessity of an electrophilic activation of the dihydropyrimidine moiety to make possible the cyclization process, a simple acid catalyst model in which the N4 nitrogen of the dihydropyrimidines **13** was protonated, was considered (see Scheme 6). This reduced model allowed to perform a comparative study of the effects of the substitution on the cyclization step, as well as to study the diastereoselectivity found at the cyclizations of **5Ac**. Thus, one TSs, **TS5**, and two intermediates, **19** and **20**, for each reaction model were studied and characterized. The total energies in gas-phase and in DMSO are given in Table 1, while a schematic representation for the reaction profiles of the acid catalyzed reactions is given in Figure 7.

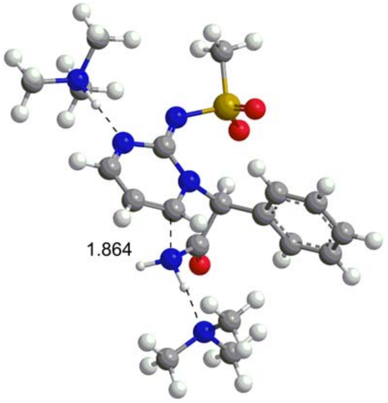

TS4

Figure 6. Transition structure, **TS4**, associated with the acid/base catalyzed cyclization of the dihydropyrimidine **13b**. The distance is given in Å.

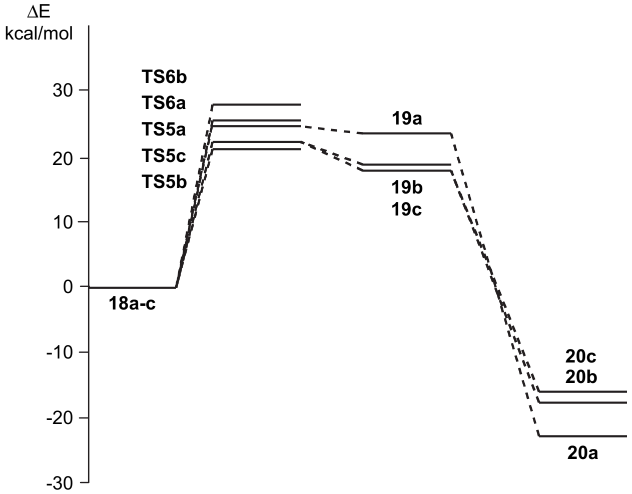

Figure 7. Reaction profiles, in DMSO, for the acid catalyzed cyclization reactions of the dihydropyrimidines **13a** and **b**.

The activation energies associated with the three cyclization models are 24.8 (32.0) kcal/mol for **TS5a**, 21.3 (24.5) kcal/mol for **TS5b**, and 22.0 (22.7) kcal/mol for **TS5c**. These values are closer to that obtained for the cyclization of the iminium cation **6** via **TS1**. These energy results indicate the requirement of a strong electrophilic activation of these dihydropyrimidines to make feasible the corresponding Michael addition. The presence of the phenyl substituent on the α position of the amide group decreases the activation energy of **TS5b** by 3.5 (7.5) kcal/mol relative to **TS5a**. Note that the effect of the phenyl substitution is larger in gas-phase. These acid catalyzed cyclization reactions are strongly endothermic, between 18 and 24 kcal/mol. However, the proton transfer process from the amide N7 nitrogen in **19** to the amine N2 one in **20** does these catalyzed processes exothermic in −16 to −23 kcal/mol (see Fig. 7).

The geometries of TSs are given in Figure 8. The length of the C1–N7 forming bond at the TSs is 1.757 Å at **TS5a**, 1.826 Å at **TS5b**, and 1.939 Å at **TS5b**. There is an increase of the length with the decrease of the gas-phase relative energy of the TS. At **TS5b** the C1–N7 length is closer to that for **TS1**. At the intermediates **19** and **20** the C1–N7 length is 1.618 and 1.444 Å at the *Model I*, 1.593 and 1.445 Å at the *Model II*, and 1.539 and 1.443 Å at the *Model III*. The C1–N7 lengths at the protonated amides **19** are larger than at protonated amines **20**, in clear agreement with the strong endothermic character of the intermediates **19**. The BO values of the C1–N7 forming bond at the TSs

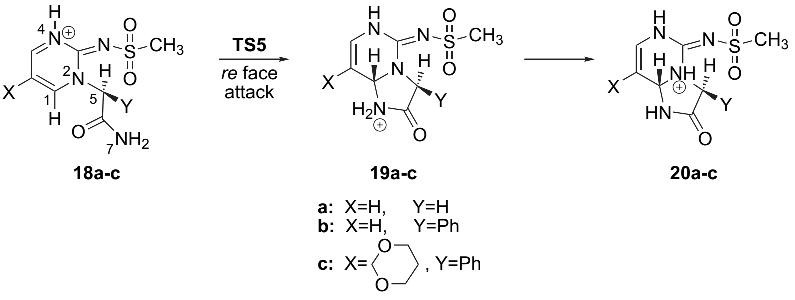

Scheme 6.

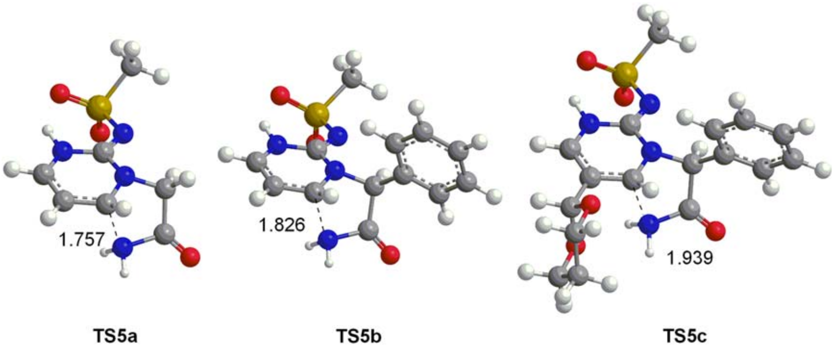

Figure 8. Transition structures, **TS5a–c**, associated with the acid catalyzed cyclizations of the dihydropyrimidines **13a** and **b**. The distances are given in Å.

are 0.61 at **TS5a**, 0.55 at **TS5b**, and 0.45 at **TS5c**. With the phenyl and dioxane substitutions, the TS for the cyclization becomes more earlier. This is in agreement with the lesser endothermic character of the corresponding protonated amide intermediate **19**.[18]

3.3.1. Study of the diastereoselectivity of the cyclization of the dihydropyrimidine 13c. The X-ray crystallographic analysis of a single crystal of **5Ac** confirmed unequivocally the structure and also the stereochemistry of the cyclization. The trans disposition of the hydrogen atoms attached to C1 and C5 indicates that the Michael addition is diastereoselective with the nucleophilic attack of the amide nitrogen occurring preferentially over the *re*-face of the planar C1 carbon (see Scheme 6). In order to explain the diastereoselectivity of this reaction, the TSs associated with the cyclization of **18a** and **18b** over the *si*-face of the planar C1 carbon were studied (see Scheme 7). The total energies in gas-phase and in DMSO are summarized in Table 1.

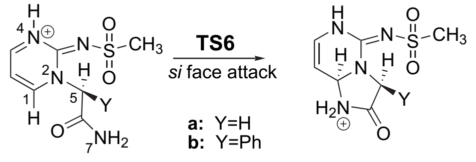

18a,b **21a,b**

Scheme 7.

The activation energies associated with **TS6a** and **TS6b** are 25.1 (33.8) and 27.9 (30.9) kcal/mol. In DMSO, these TSs are 0.3 and 6.6 kcal/mol higher in energy than **TS5a** and **TS5b**, respectively (see Fig. 7). Thus, while in the absence of the phenyl group both diastereoisomeric TSs have similar energies, in the presence of the phenyl group on C5, the ring closure caused by the attack over the *si*-face is 6.6 kcal/mol higher in energy than the attack over the *re*-face, in clear agreement with the complete diastereoselectivity observed in the cyclization of the dihydropyrimidine **1Ac**. The low difference found at **TS6a** can be associated with the unlike conformations adopted by the cyclic five-membered **TS5a** and **TS6a**.

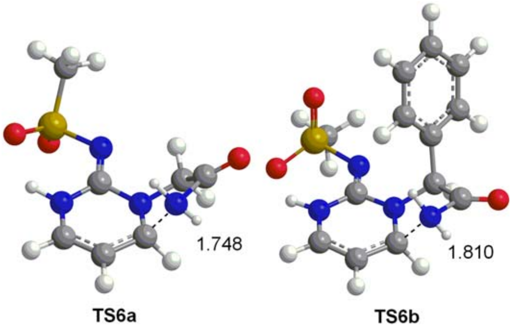

Figure 9. Transition structures, **TS6a** and **b**, associated with the diastereoisomeric paths of the acid catalyzed cyclizations of the dihydropyrimidines **13a** and **b**. The distances are given in Å.

The geometries of the two diastereoisomeric TSs are given in Figure 9. The length of the C1–N7 forming bond at these TSs are 1.748 (**TS6a**) and 1.810 (**TS6b**) Å. These values are slightly shorter than that at the two diastereoisomeric TSs **TS5a** and **TS5b**. Analysis of the geometry of **TS6b** indicates that the methanesulfonyl group is located over the plain of the phenyl group. The distance between both groups is of 3.8 Å. Therefore, the unfavorable interactions that appear between both groups at **TS6b**, which are absent at **TS5b**, are responsible for the diastereoselectivity found at the cyclization of **1Ac**. Finally, the BO values of the C1–N7 forming bond at these TSs are 0.63 (**TS6a**) and 0.56 (**TS6b**).

3.4. Analysis of the electrophilicity of the Michael acceptors

A recent study carried out on electrophilically activated C–C double bonds has shown that the analysis of the electrophilicity index, ω, is a powerful tool to analyze the participation of the C–C double bond in nucleophilic addition reactions such as the Michael addition.[19] Thus, the electrophilicity of some compounds related to these intramolecular cyclizations has been analyzed. In Table 2, the global reactivity indexes are given.

The α,β-unsaturated imine **24** has an electrophilicity value ω of 1.10 eV (see Table 2). It is classified as a moderate electrophile within the electrophilicity scale.[20] The dihydropyrimidine **13a** has electrophilicity value of 2.26 eV. Although it is classified as a strong electrophile, its relatively low value indicates that it will participate as Michael acceptor only toward strong nucleophiles. Note that the amide is a very poor nucleophile.

Protonation of the nitrogen atom of the imine **24** strongly increases notably the electrophilicity of iminium cation **22**,

Table 2. Global indexes of some Michael-type acceptors

	μ (au)	η (au)	ω (eV)
18a	−0.3364	0.1414	10.89
22	−0.3383	0.1810	8.60
6	−0.3318	0.1804	8.30
23	−0.3070	0.1919	6.68
13a	−0.1622	0.1586	2.26
24	−0.1281	0.2024	1.10

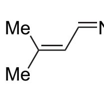

24

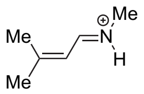

22

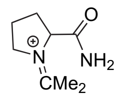

23

ω=8.60 eV. This value is closer to that for the cyclic iminium cation **6**, 8.30 eV, for which the activation energy for the cyclization has been estimated in 21.4 kcal/mol. Note that methyl substitution on the terminal methylene of **6** decreases the electrophilicity of **23** to 6.68 eV, as a consequence of the electron-releasing character of the methyl groups.

Finally, protonation of the N4 nitrogen atom of the dihydropyrimidine **13a** increases the electrophilicity of **18a** to 10.89 eV, being the stronger electrophile of the series given in Table 2. This strong electrophilic activation of the pyrimidine ring accounts for the acid catalysis demanded for the cyclization of these dihydropyrimidines.

4. Conclusions

The transformation of 2-(2-sulfonylimino-1,2-dihydro-1-pyrimidinyl) acetamides into imidazo[1,2-*c*]pyrimidines through a ring closure reaction has been studied using DFT calculations at the B3LYP/6-31G* level. Calculations carried out on the neutral species indicate that the cyclization step has very high activation energy as a consequence of the low electrophilic character of the dihydropyrimidine moiety and the very low nucleophilic character of the appended amide. In addition, the solitary base catalysis is not sufficient to allow the cyclization process, being necessary an acid. This acid catalysis allows the intramolecular Michael addition by a strong electrophilic activation of the α,β-unsaturated imine system present on the dihydropyrimidine ring. In addition, the substitution on both dihydropyrimidine and amide moieties has also an influence on the activation energy associated with the cyclization process. Thus, the presence of the phenyl group on the amide, reduces the activation energies as well makes the cyclization to be diastereoselective.

Analysis of the electrophilicity index at some reagents involved in these cyclizations allows an understanding of the role of the acid catalyst. We can conclude that, although the carboxamide group can act as nucleophile and the α,β-unsaturated imine residue of the dihydropyrimidine ring can act as electrophile, a strong electrophilic activation of the dihydropyrimidine ring is necessary in order to make possible the corresponding intramolecular Michael addition.

Acknowledgements

This work was supported by research funds provided by the Universidad de Valencia (project UV-AE-06-3). J.A.S. thanks to the Ministerio de Ciencia y Tecnología for his doctoral fellowship.

References and notes

1. Acero-Alarcón, A.; Armero-Alarte, T.; Jordá-Gregori, J. M.; Rojas-Argudo, C.; Zaballos-García, E.; Server-Carrió, J.; Ahjyaje, F. Z.; Sepulveda-Arques, J. *Synthesis* **1999**, 2124–2130.
2. (a) Sliskovic, D. R. *Comprehensive Heterocyclic Chemistry*; Katrizky, A. R., Rees, C. W., Scriven, E. F., Eds.; Pergamon: Oxford, 1996; Vol. 8, p 354; (b) Katritzky, A. R.; Xu, Y.-J.; Tu, H. *J. Org. Chem.* **2003**, *68*, 4935–4937.
3. (a) Kukla, M. J.; Breslin, H. J. *J. Org. Chem.* **1987**, *52*, 5046–5048; (b) Panetta, C. A.; Pesh-Imam, M. *J. Org. Chem.* **1972**, *37*, 302–304.
4. (a) Federsel, H.-J.; Könberg, E.; Lilljequist, L.; Swahn, B.-M. *J. Org. Chem.* **1990**, *55*, 2254–2256; (b) Polonski, T. *Tetrahedron* **1985**, *41*, 611–616.
5. Gottstein, W. J.; Minor, W. F.; Cheney, L. C. *J. Am. Chem. Soc.* **1958**, *81*, 1198–1201.
6. (a) Becke, A. D. *J. Chem. Phys.* **1993**, *98*, 5648–5652; (b) Lee, C.; Yang, W.; Parr, R. G. *Phys. Rev. B* **1988**, *37*, 785–789.
7. Hehre, W. J.; Radom, L.; Schleyer, P. vR.; Pople, J. A. *Ab initio Molecular Orbital Theory*; Wiley: New York, NY, 1986.
8. (a) Schlegel, H. B. *J. Comput. Chem.* **1982**, *3*, 214–218; (b) Schlegel, H. B. Geometry Optimization on Potential Energy Surface. In *Modern Electronic Structure Theory*; Yarkony, D. R., Ed.; World Scientific Publishing: Singapore, 1994.
9. Fukui, K. *J. Phys. Chem.* **1970**, *74*, 4161–4163.
10. (a) González, C.; Schlegel, H. B. *J. Phys. Chem.* **1990**, *94*, 5523–5527; (b) González, C.; Schlegel, H. B. *J. Chem. Phys.* **1991**, *95*, 5853–5860.
11. (a) Reed, A. E.; Weinstock, R. B.; Weinhold, F. *J. Chem. Phys.* **1985**, *83*, 735–746; (b) Reed, A. E.; Curtiss, L. A.; Weinhold, F. *Chem. Rev.* **1988**, *88*, 899–926.
12. Frisch, M. J.; Trucks, G. W.; Schlegel, H. B.; Scuseria, G. E.; Robb, M. A.; Cheeseman, J. R.; Montgomery, J. A., Jr.; Vreven, T.; Kudin, K. N.; Burant, J. C.; Millam, J. M.; Iyengar, S. S.; Tomasi, J.; Barone, V.; Mennucci, B.; Cossi, M.; Scalmani, G.; Rega, N.; Petersson, G. A.; Nakatsuji, H.; Hada, M.; Ehara, M.; Toyota, K.; Fukuda, R.; Hasegawa, J.; Ishida, M.; Nakajima, T.; Honda, Y.; Kitao, O.; Nakai, H.; Klene, M.; Li, X.; Knox, J. E.; Hratchian, H. P.; Cross, J. B.; Adamo, C.; Jaramillo, J.; Gomperts, R.; Stratmann, R. E.; Yazyev, O.; Austin, A. J.; Cammi, R.; Pomelli, C.; Ochterski, J. W.; Ayala, P. Y.; Morokuma, K.; Voth, G. A.; Salvador, P.; Dannenberg, J. J.; Zakrzewski, V. G.; Dapprich, S.; Daniels, A. D.; Strain, M. C.; Farkas, O.; Malick, D. K.; Rabuck, A. D.; Raghavachari, K.; Foresman, J. B.; Ortiz, J. V.; Cui, Q.; Baboul, A. G.; Clifford, S.; Cioslowski, J.; Stefanov, B. B.; Liu, G.; Liashenko, A.; Piskorz, P.; Komaromi, I.; Martin, R. L.; Fox, D. J.; Keith, T.; Al-Laham, M. A.; Peng, C. Y.; Nanayakkara, A.; Challacombe, M.; Gill, P. M. W.; Johnson, B.; Chen, W.; Wong, M. W.; Gonzalez, C.; Pople, J. A. *Gaussian 03, Revision C.02*; Gaussian, Inc.: Wallingford, CT, 2004.

13. (a) Tomasi, J.; Persico, M. *Chem. Rev.* **1994**, *94*, 2027–2094; (b) Simkin, B. Y.; Sheikhet, I. *Quantum Chemical and Statistical Theory of Solutions—A Computational Approach*; Ellis Horwood: London, 1995.
14. (a) Cances, E.; Mennucci, B.; Tomasi, J. *J. Chem. Phys.* **1997**, *107*, 3032–3041; (b) Cossi, M.; Barone, V.; Cammi, R.; Tomasi, J. *Chem. Phys. Lett.* **1996**, *255*, 327–335; (c) Barone, V.; Cossi, M.; Tomasi, J. *J. Comput. Chem.* **1998**, *19*, 404–417.
15. Parr, R. G.; Pearson, R. G. *J. Am. Chem. Soc.* **1983**, *105*, 7512–7516.
16. (a) Parr, R. G.; Yang, W. *Density Functional Theory of Atoms and Molecules*; Oxford University Press: New York, NY, 1989; (b) Parr, R. G.; von Szentpaly, L.; Liu, S. *J. Am. Chem. Soc.* **1999**, *121*, 1922–1924.
17. Wiberg, K. B. *Tetrahedron* **1968**, *24*, 1083–1096.
18. Hammond, G. S. *J. Am. Chem. Soc.* **1955**, *77*, 334–338.
19. Domingo, L. R.; Perez, P.; Contreras, R. *Tetrahedron* **2004**, *60*, 6585–6591.
20. Domingo, L. R.; Aurell, M. J.; Pérez, P.; Contreras, R. *Tetrahedron* **2002**, *58*, 4417–4423.